Time Domain Finite Difference Methods for Range Dependent Biot Media

Ralph Stephen

Woods Hole Oceanographic Institution (MS#24)
360 Woods Hole Road
Woods Hole, MA 02543-1542, USA
Email: rstephen@whoi.edu

Abstract

The physics of sound propagation in saturated, porous (Biot) media differs from propagation in fluids and elastic/anelastic solids because of the existence of a second compressional wave, the "slow" wave. Many environments in bottom interacting ocean acoustics consist of mud and sands which can be modeled as saturated, porous solids with low shear moduli. In order to understand the physical mechanisms responsible for acoustic propagation, attenuation, and scattering in these processes, we have extended our Numerical Scattering Chamber code to solve Biot's equations in two dimensional Cartesian coordinates. The NSC formulation is based on the method of time domain finite differences and is applicable to the rough and laterally heterogeneous structures that are found on the seafloor. Within the same code we can compare acoustic, elastic, anelastic and Biot models for realistic environments with subbottom heterogeneities and seafloor roughness with scale lengths comparable to acoustic wavelengths. All multiple interactions and mode conversions are included in the solution.

1. Introduction

Chotiros [1] outlined three cases where Biot's theory for wave propagation in porous media could be applied to the interpretation of bottom interacting acoustic data. He postulated that the existence of the Biot slow wave was necessary to interpret the energy partitioning of an acoustic beam on a water to water-saturated sand interface. If slow waves play an important role at flat interfaces between homogeneous media, what role do they play in forward and back scattering from rough interfaces or from sub-bottom heterogeneities? Time domain finite differences have proven to be a useful tool in identifying the physical processes responsible for scattering from elastic and anelastic seafloors [2-4]. We are developing a time domain finite difference code to study the additional mechanisms that may be introduced in saturated porous media.

Time domain finite difference methods have a number of advantages over other methods for simulating bottom scattering. Time domain solutions to the two-way wave equations contain all multiple interactions between scatterers, including all mode conversions between compressional (fast and slow), shear and interface waves. Interface roughness and sub-bottom heterogeneities, with length scales on the order of acoustic wavelengths, can be studied with the same methodology. Models can consist of arbitrary combinations of acoustic, elastic, anelastic and poro-elastic media. Wavefront snapshots, in addition to time series at arbitrary locations within the model, provide useful insights into the propagation and scattering of sound in complex media.

2. The Method

2.1 Biot's Equations for Heterogeneous Media with Non-Uniform Porosity

Biot [5] (Equation 8.24) gives the wave equation for a heterogeneous, non-uniform porosity, poro-elastic medium:

$$
\begin{aligned}
&2\sum_j \frac{\partial}{\partial x_j}\left(\mu e_{ij}\right)+\frac{\partial}{\partial x_i}\left(\lambda_c e-\alpha M\zeta\right)=\frac{\partial^2}{\partial t^2}\left(\rho u_i+\rho_f w_i\right)\\
&\frac{\partial}{\partial x_i}\left(\alpha M e-M\zeta\right)=\frac{\partial^2}{\partial t^2}\left(\rho_f u_i+m w_i\right)+\frac{\eta}{k}\frac{\partial w_i}{\partial t}
\end{aligned}
\tag{1}
$$

where μ, λ_c, α and M are poro-elastic parameters, u_i and U_i are displacement vectors for the solid and fluid components respectively, f is porosity, η is the fluid viscosity, k is the permeability, ρ_f is the fluid density, ρ is the total mass of bulk material per unit volume, and m is a third mass parameter. Also:

$$
\begin{aligned}
&\mathbf{w}=f(\mathbf{U}-\mathbf{u})\\
&\zeta=-div[\mathbf{w}]\\
&e=div[\mathbf{u}]\\
&e_{ij}=\begin{Bmatrix}
\dfrac{\partial u_x}{\partial x} & \dfrac{1}{2}\left(\dfrac{\partial u_y}{\partial x}+\dfrac{\partial u_x}{\partial y}\right) & \dfrac{1}{2}\left(\dfrac{\partial u_z}{\partial x}+\dfrac{\partial u_x}{\partial z}\right)\\
\dfrac{1}{2}\left(\dfrac{\partial u_y}{\partial x}+\dfrac{\partial u_x}{\partial y}\right) & \dfrac{\partial u_y}{\partial y} & \dfrac{1}{2}\left(\dfrac{\partial u_y}{\partial z}+\dfrac{\partial u_z}{\partial y}\right)\\
\dfrac{1}{2}\left(\dfrac{\partial u_z}{\partial x}+\dfrac{\partial u_x}{\partial z}\right) & \dfrac{1}{2}\left(\dfrac{\partial u_y}{\partial z}+\dfrac{\partial u_z}{\partial y}\right) & \dfrac{\partial u_z}{\partial z}
\end{Bmatrix}
\end{aligned}
\tag{2}
$$

Note that just about all other equations in Biot's porous media papers, including all of the familiar equations, assume uniform porosity and homogeneous material. In our finite difference approach we rely on gradients of elastic parameters (and porosity) to compute the effects of interfaces. We do not introduce boundary conditions explicitly. So it is important to have the correct equations for heterogeneous, non-uniform porosity material. A finite difference solution to Biot's equation 8.25 for a homogeneous, uniform porosity, medium was treated by Zhu and McMechan [6]. Hassanzadeh [7] presented solutions to Biot's equations for dilatational waves in a homogeneous, uniform porosity medium ([8], equation 7.1). Neither of these approaches is satisfactory for our applications.

Following Biot [5] (1) can be rewritten in a form similar to Biot's equation 8.25 but valid for heterogeneous, non-uniform porosity material:

$$
\begin{aligned}
&\mu\nabla^2\mathbf{u}+(\mu+\lambda_c)\nabla e-\alpha M\nabla\zeta+\nabla\mu\cdot\left[\nabla\mathbf{u}+(\nabla\mathbf{u})^T\right]+\nabla\lambda_c e-\nabla(\alpha M)\zeta\\
&\qquad=\frac{\partial^2}{\partial t^2}\left(\rho\mathbf{u}+\rho_f\mathbf{w}\right)\\
&\nabla\left(\alpha M e-M\zeta\right)=\frac{\partial^2}{\partial t^2}\left(\rho_f\mathbf{u}+m\mathbf{w}\right)+\frac{\eta}{k}\frac{\partial\mathbf{w}}{\partial t}
\end{aligned}
\tag{3}
$$

Also, the more familiar form of Biot's equation 8.1 becomes for a heterogeneous, non-uniform porosity material:

$$
\begin{aligned}
&N\nabla^2\mathbf{u}+(N+A)\nabla e+Q\nabla\varepsilon \\
&+\frac{Q}{f}\left\{\nabla\left[\nabla f\cdot(\mathbf{u}-\mathbf{U})\right]+\nabla f(e-\varepsilon)\right\}+\nabla\mu\cdot\left[\nabla\mathbf{u}+(\nabla\mathbf{u})^T\right] \\
&+\left[\nabla\lambda_c-f\nabla(\alpha M)\right]e-\left[\nabla(\alpha M)-f\nabla M\right]\left[\nabla f\cdot(\mathbf{u}-\mathbf{U})+f(e-\varepsilon)\right] \\
&\qquad=\frac{\partial^2}{\partial t^2}(\rho_{11}\mathbf{u}+\rho_{12}\mathbf{U})+b\frac{\partial}{\partial t}(\mathbf{u}-\mathbf{U}) \\
&f\left[\nabla\left(\frac{Q}{f}e+\frac{R}{f}\varepsilon\right)+\nabla\left\{\frac{R}{f^2}\left[\nabla f\cdot(\mathbf{U}-\mathbf{u})\right]\right\}\right] \\
&=\frac{\partial^2}{\partial t^2}(\rho_{12}\mathbf{u}+\rho_{22}\mathbf{U})-b\frac{\partial}{\partial t}(\mathbf{u}-\mathbf{U})
\end{aligned}
\tag{4}
$$

where from Biot's equations 8.19, 8.2 and 3.31 (low frequency approximation):

$$
\begin{aligned}
\rho_{11}&=\rho-2\rho_f f+mf^2 \\
\rho_{22}&=mf^2 \\
\rho_{12}&=\rho_f f-mf^2 \\
b&=\frac{\eta}{k}f^2 \\
Q&=f(\alpha-f)M \\
R&=f^2M \\
N&=\mu \\
A&=\lambda_c-2\alpha fM+Mf^2
\end{aligned}
\tag{5}
$$

Alternatively, in terms of the porosity weighted pressure in the fluid, s=-fp, and the volume averaged stress tensor for the solid, Σ, (1) can be expressed as a coupled system of the equations of motion [9]:

$$
\begin{aligned}
\rho_{11}\frac{\partial^2\mathbf{u}}{\partial t^2}+\rho_{12}\frac{\partial^2\mathbf{U}}{\partial t^2}&=\nabla\cdot\Sigma+b\frac{\partial}{\partial t}(\mathbf{U}-\mathbf{u}) \\
\rho_{12}\frac{\partial^2\mathbf{u}}{\partial t^2}+\rho_{22}\frac{\partial^2\mathbf{U}}{\partial t^2}&=\nabla s-b\frac{\partial}{\partial t}(\mathbf{U}-\mathbf{u})
\end{aligned}
\tag{6}
$$

and the stress-strain relations in terms of displacement:

$$s = Q\nabla\cdot\mathbf{u} + R\nabla\cdot\mathbf{U} + \frac{R}{f}\nabla f\cdot(\mathbf{U}-\mathbf{u})$$
$$\Sigma = N\left[\nabla\mathbf{u} + (\nabla\mathbf{u})^T\right] + \left[A\nabla\cdot\mathbf{u} + Q\nabla\cdot\mathbf{U} + \frac{Q}{f}\nabla f\cdot(\mathbf{U}-\mathbf{u})\right]\mathbf{I} \tag{7}$$

where $\mathbf{I}$ is the identity matrix. Note that contrary to elasticity, in poro-elasticity the infinitesimal cube over which the stresses and strains are defined is not homogeneous. It is necessary to consider the gradients in porosity in the stress-strain relation. On comparing (6) to (4) it would appear that the first and second equations in (4) should correspond to $\cdot\Sigma$ and s respectively but they do not. The discrepancy has not been resolved. Equations(6) and (7) are equivalent to equation (4), however, when porosity is uniform (f=0). The equations in this case which are valid for heterogeneous, uniform-porosity material are:

$$\begin{aligned}&(A+N)\nabla(\nabla\cdot\mathbf{u}) + N\nabla^2\mathbf{u} + Q\nabla(\nabla\cdot\mathbf{U}) + \nabla A(\nabla\cdot\mathbf{u})\\ &+\nabla N\times(\nabla\times\mathbf{u}) + 2(\nabla N\cdot\nabla)\mathbf{u} + \nabla Q(\nabla\cdot\mathbf{U})\\ &= \frac{\partial^2}{\partial t^2}(\rho_{11}\mathbf{u} + \rho_{12}\mathbf{U}) + b\frac{\partial}{\partial t}(\mathbf{u}-\mathbf{U})\end{aligned} \tag{8}$$

$$\begin{aligned}&Q\nabla(\nabla\cdot\mathbf{u}) + R\nabla(\nabla\cdot\mathbf{U}) + \nabla Q(\nabla\cdot\mathbf{u}) + \nabla R(\nabla\cdot\mathbf{U})\\ &= \frac{\partial^2}{\partial t^2}(\rho_{12}\mathbf{u} + \rho_{22}\mathbf{U}) - b\frac{\partial}{\partial t}(\mathbf{u}-\mathbf{U})\end{aligned}$$

A finite difference solution to these equations was presented by Stephen [10]. A solution to these equations, valid for uniform porosity media, is discussed below.

2.2 Approximations and Assumptions

In establishing the wave equations for poro-elastic media Biot made the following assumptions [9]. Disconnected pores are treated as part of the solid matrix. The porous medium is macroscopically isotropic. The pore size is much less than all geoacoustic wavelengths. Deformations are small so that the differential equations will be linear. The force of gravity and temperature variations are neglected. A low frequency approximation is made so that the flow between the pores can be considered Poïseuille type.

In applying our finite difference approach to these equations we make further assumptions. All of the parameters are assumed to be frequency independent over the bandwidth of the source, which is an octave in pressure in our examples. We do not include intrinsic anelasticity for the solid frame. We solve the poro-elastic equations for a point source in a two dimensional, Cartesian geometry. We neglect porosity gradients in the stress-strain relation so the code is appropriate for only slowly varying porosity.

3. An Example

For testing purposes we consider as an example a point source in a poro-elastic layer between an acoustic half-space and an elastic half-space (Figure 1). The parameters for the poro-elastic medium represent a water saturated sand [11] without intrinsic attenuation (Table 1). Our values differ slightly from [11]. Our bulk modulus of the fluid corresponds to a water velocity of 1500m/s. Also we chose a very small permeability to initially test the code without the viscous coupling term.

Table 1: Parameters for the poro-elastic layer in Figure 1.

Porosity	f	0.47	
Viscosity	η	10^{-6}	kg/(m-s)
Permeability	k	10^{-10}	m^2
Fluid Density	ρ_f	10^3	kg/m^3
Solid Grain Density	ρ_s	2650	kg/m^3
Grain Bulk Modulus	K_s	$3.6x10^{10}$	Pa
Fluid Bulk Modulus	K_f	$2.25x10^9$	Pa
Dry Skeleton Bulk Modulus	K_B	$4.36x10^7$	Pa
Dry Skeleton Shear Modulus	N	$2.61x10^7$	Pa

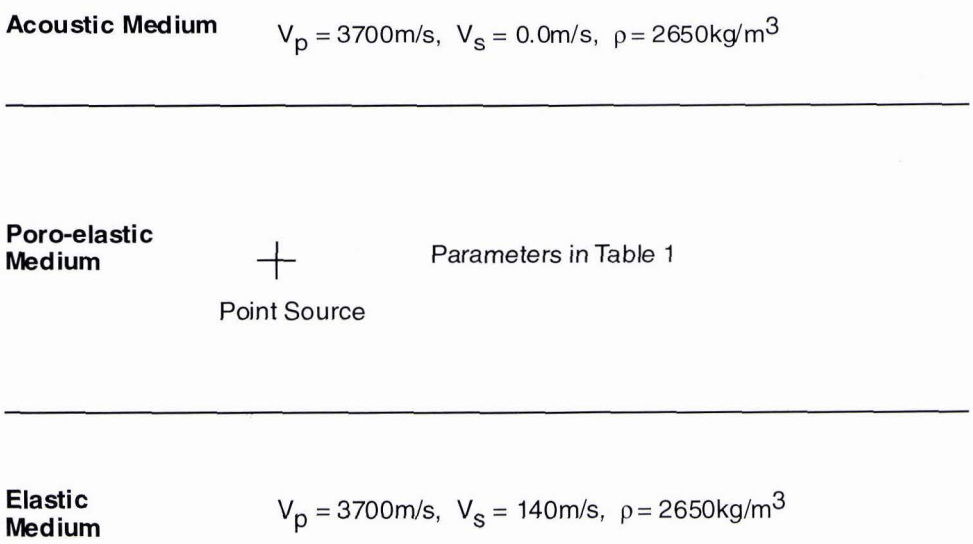

Figure 1: For testing purposes we consider a poro-elastic layer between an acoustic half-space and an elastic half-space.

The parameters required in (8) can be expressed in terms of the parameters in Table 1:

$$A = \frac{(1-f)\left(1-f-\frac{K_b}{K_s}\right)K_s + f\frac{K_s}{K_f}K_b}{1-f-\frac{K_b}{K_s}+f\frac{K_s}{K_f}} - \frac{2}{3}N$$

$$Q = \frac{\left(1-f-\frac{K_b}{K_s}\right)fK_s}{1-f-\frac{K_b}{K_s}+f\frac{K_s}{K_f}} \qquad (9)$$

$$R = \frac{f^2 K_s}{1-f-\frac{K_b}{K_s}+f\frac{K_s}{K_f}}$$

$$\rho_{11} = (1-f)\rho_s + \tfrac{1}{3}f\rho_f$$

$$\rho_{12} = -\tfrac{1}{3}f\rho_f$$

$$\rho_{22} = \tfrac{4}{3}f\rho_f$$

The source time series in pressure is the third derivative of a Gaussian curve with a peak frequency of 400Hz. The time increment is 1/400th of a period at the peak frequency. The spatial sampling is 1/280th of a compressional wavelength at the peak frequency in pressure in the acoustic medium. This corresponds to sampling the shear waves in the lower medium at 10 points/wavelength. For testing we chose the compressional velocity and density of the upper acoustic medium and the lower elastic medium to match the compressional velocity and density of the poro-elastic layer when the porosity is zero. Obviously more realistic values for the compressional velocity and density of the upper acoustic medium would be 1500m/s and 1000kg/m^3, corresponding to water. For this case the spatial sampling would be about 114 points per wavelength. Since all times and distances in the calculation scale proportional to inverse frequency the output can be specified in periods and compressional wavelengths in the acoustic medium.

Figure 2 shows a snapshot at 7.5Periods after the initiation of the source pulse for a layer thickness of 1.82 wavelengths with the source at a depth of about 0.9wavelengths. The top frame labeled 'compressional' corresponds to a scaled version of the divergence of the solid displacement vector. The lower frame corresponds to the curl of the solid displacement vector. At this stage we have not confirmed the validity of the amplitudes. Kinematically however we can see the wavefronts corresponding to the direct, surface reflected and bottom reflected fast compressional waves to the right of the upper figure. The slow wave generated at the source is the circular wavefront on the left of the upper figure. The short wavelength bottom reflection corresponds kinematically to a converted slow wave but the amplitudes have not been tested. Since the formulation assumed uniform porosity it is unlikely that the converted slow wave is correct.

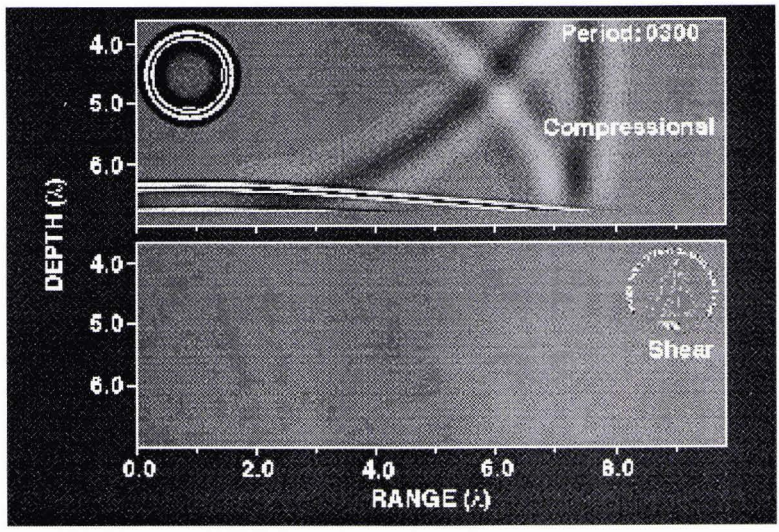

Figure 2: Snapshots of the divergence (top) and curl (bottom) of the solid displacement vector 7.5 periods after the source pulse was initiated in the test model.

4. Conclusions

This paper is a progress report of on-going research. Further validity testing for homogeneous, porous media is clearly required. We recommend that benchmarks be established for porous media problems. Using a Gaussian pulse-beam rather than a point source will limit the wave number content of the incident field while restricting the computational domain. Ultimately the code should be applied to analysis of actual field data.

The time domain finite difference method is a promising technique for addressing the physical mechanisms of forward and back scattering from range dependent porous media with interface roughness and/or volume (sub-bottom) heterogeneities. Wavefront snapshots provide insight into the conversion between fast, slow and shear waves at interfaces between homogeneous poro-elastic and elastic layers. Within the Numerical Scattering Chamber methodology one can address a broad range of scattering problems for acoustic, elastic, anelastic and poro-elastic media.

5. Acknowledgements

The work described in this paper was supported by the Office of Naval Research under Contract Number N00014-96-1-0460.

References

[1] N. P. Chotiros, "Biot model of sound propagation in water-saturated sand," *J. acoust. Soc. Am.*, vol. 97, pp. 199-214, 1995.

[2] R. A. Stephen and S. A. Swift, "Finite difference modeling of geoacoustic interaction at anelastic seafloors," *J. acoust. Soc. Am.*, vol. 95, pp. 60-70, 1994.

[3] R. A. Stephen and S. A. Swift, "Modeling seafloor geoacoustic interaction with a numerical scattering chamber," *J. acoust. Soc. Am.*, vol. 96, pp. 973-990, 1994.

[4] S. A. Swift and R. A. Stephen, "The scattering of a low-angle pulse beam by seafloor volume heterogeneities," *J. acoust. Soc. Am.*, vol. 96, pp. 991-1001, 1994.

[5] M. A. Biot, "Mechanics of deformation and acoustic propagation in porous media," *J. appl. phys.*, vol. 33, pp. 1482-1488, 1962.

[6] X. Zhu and G. A. McMechan, "Numerical simulation of seismic responses of poroelastic reservoirs using Biot theory," *Geophysics*, vol. 56, pp. 328-339, 1991.

[7] S. Hassanzadeh, "Acoustic modeling in fluid-saturated porous media," *Geophysics*, vol. 56, pp. 424-435, 1991.

[8] M. A. Biot, "Theory of propagation of elastic waves in a fluid saturated porous solid. I. Low-frequency range," *J. acoust. Soc. Am.*, vol. 28, pp. 168-178, 1956.

[9] N. Dai, A. Vafidis, and E. R. Kanasewich, "Wave propagation in heterogeneous, porous media: A velocity-stress, finite-difference method," *Geophysics*, vol. 60, pp. 327-340, 1995.

[10] R. A. Stephen, "A finite difference formulation of Biot's equations for vertically heterogeneous full waveform acoustic logging problems," in *Full Waveform Acoustic Logging Consortium Annual Report*, M. N. Toksöz and C. H. Cheng, Eds. Boston: Massachusetts Institute of Technology Earth Resources Laboratory, 1987, pp. 115-123.

[11] R. D. Stoll and T. K. Kan, "Reflection of acoustic waves at a water-sediment interface," *J. acoust. Soc. Am.*, vol. 70, pp. 149-156, 1981.